

## The Electronic Spectra and the Intermolecular Interaction of Würster's Ions in Crystals

Jiro TANAKA and Masagi MIZUNO<sup>\*1</sup>

*Department of Chemistry, Faculty of Science, Nagoya University, Chikusa-ku, Nagoya*

(Received November 30, 1968)

The electronic spectra and the intermolecular interaction of Würster's radical have been studied for the dimer state and for the crystalline states. The polarization properties of the excited states have been investigated in detail, and the longest wavelength absorption band of the dimer has been established as having a charge-transfer character. The strength of the charge-transfer band and the shift of the monomer band in the dimer or in the crystalline states are shown to be intimately correlated with the strength of the intermolecular interactions between the stacked radicals. A theoretical analysis of the excited state of the dimer and the crystals is presented; the results are in good agreement with the experimental findings.

Würster's ions are well known to dimerize at lower temperatures in a solution. Hausser and Murrell<sup>1)</sup> first pointed out that the origin of the longest-wavelength absorption band of the dimer is charge-transfer in nature and suggested that the ions might be stacked on each other in a solution. Suzuki, Ooshika, and their coworkers<sup>2)</sup> extended the earlier work and found the equilibrium constant for dimerization. A similar line of experiment was carried out by Kimura, Yamada, and Tsubomura<sup>3)</sup> recently. Kommandeur and Pott<sup>4)</sup> discussed the nature of the electronic transition from a different viewpoint and suggested that a doubly-charged cation and a neutral molecule might be involved in the appearance of the longest-wavelength band. On the other hand, McConnell and his group,<sup>5)</sup> however, insisted on the charge-transfer mechanism and a recent experiment by Sakata and Nagakura<sup>6)</sup> has also supported this interpretation.

In this laboratory an X-ray structure analysis has been carried out on several Würster's salts,<sup>7)</sup>

and a combined investigation of the spectra and structure of the crystals has been attempted. The measurement of the absorption spectra with a single crystal by means of polarized light is the most reliable method for confirming the symmetry properties of the excited state if the crystal structure has already been established. In this paper we will present: (1) a theoretical treatment of the dimer interaction, (2) the findings on the crystalline absorption spectra of various Würster's salts, and (3) a discussion of the nature of the electronic transition in the crystalline state.

The longest-wavelength absorption bands of the crystals have definitely been determined to be an intermolecular charge-transfer between the stacked radicals. The appearance of the charge-transfer band in the crystalline spectra is intimately correlated with the magnitude of the intermolecular electron exchange interaction, which can be estimated by means of the overlap integrals between the molecular orbitals of the radicals. The polarization properties of the radical excited states have been determined; the findings are supported by the theoretical analysis<sup>8)</sup> of the radical spectra. The configurational mixing between the charge-transfer state with the local excited state shifts the visible band of the radical to a shorter wavelength. It may be concluded that the electron-exchange effect between the radicals is most important in determining the optical and other electronic properties of organic free-radical crystals.

### Theory of the Dimer Interaction

According to results of the X-ray crystal structure analysis, the interplanar distances between the

8) To be published elsewhere.

<sup>\*1</sup> Present address: The Government Chemical Industrial Research Institute, Tokyo.

1) K. H. Hausser and J. N. Murrell, *J. Chem. Phys.*, **27**, 500 (1957).

2) K. Uemura, S. Nakayama, Y. Seo, K. Suzuki and Y. Ooshika, *This Bulletin*, **39**, 1348 (1966).

3) K. Kimura, H. Yamada and H. Tsubomura, *J. Chem. Phys.*, **48**, 440 (1968).

4) J. Kommandeur and G. T. Pott, *ibid.*, **47**, 395 (1967).

5) P. L. Nordio, Z. G. Soos and H. M. McConnell, *Ann. Rev. Phys. Chem.*, **17**, 237 (1966).

6) T. Sakata and S. Nagakura, *Technical Report of Institute for Solid State Physics, The University of Tokyo*, Ser. A, No. 244 (1967).

7) J. Tanaka and N. Sakabe, *Acta Cryst.*, **B24**, 1345 (1968).

stacked radicals are in the range of 3.1–3.7 Å. In the region of these intermolecular distances, covalent bondings between the radicals may be expected; their strength can be estimated by the electron overlap between the half-filled molecular orbitals of the radicals. The Heitler-London approach is most appropriate for the treatment of the inter-radical interaction at these distances, since the molecular orbital method would emphasize the electron delo-

calization effect too much. In the following treatment we will consider only the highest singly-occupied orbital as a one-electron problem and will neglect the effects of all the other occupied orbitals. The singly-occupied highest molecular orbitals of *a* and *b*th radicals are denoted by  $\phi_a^m$  and  $\phi_b^m$ , and vacant orbitals, by  $\phi_a^e$  and  $\phi_b^e$ .

The orbital wave function of the singlet state may be given as follows:

Ground Configuration:

$$\Psi_G = \frac{1}{\sqrt{2(1 + S_{mm}^2)}} [\phi_a^m(1)\phi_b^m(2) + \phi_b^m(1)\phi_a^m(2)]$$

Charge-transfer Configuration:

$$\Psi_{CT\pm} = \frac{1}{\sqrt{2(1 \pm S_{mm}^2)}} [\phi_a^m(1)\phi_a^m(2) \pm \phi_b^m(1)\phi_b^m(2)]$$

Molecular Excited Configuration:

$$\Psi_{M\pm} = \frac{1}{\sqrt{4 + 2S_{me}^2 + 2S_{mm}S_{ee}}} [\phi_a^e(1)\phi_b^m(2) + \phi_b^m(1)\phi_a^e(2) \pm \phi_a^m(1)\phi_b^e(2) \pm \phi_a^m(2)\phi_b^e(1)]$$

where the upper sign corresponds to the symmetric state and the lower one to the antisymmetric state.

The total Hamiltonian for the system is given by;

$$H = H_a + H_b + V_{ab}$$

$$H_a = -\frac{1}{2}\nabla_1^2 - \sum_i \delta_i / R_{a_i1}$$

$$H_b = -\frac{1}{2}\nabla_2^2 - \sum_j \delta_j / R_{b_j2}$$

$$V_{ab} = -\sum_j \delta_j / R_{b_j1} - \sum_i \delta_i / R_{a_i2} + 1/r_{12} + \sum_{i,j} \delta_i \delta_j / R_{a_i, b_j}$$

where  $\sum_i \delta_i R_{a_i1}$  indicates the core attraction potentials for the first electron by the *i*th atomic core of the *a*th radical with a  $\delta_i$  effective charge, which is produced by stripping off one electron from the complete radical. The molecular orbital of the radical is given by the LCAO form while the orbital energies for the isolated system are given by:

$$\phi_a^m = \sum_i C_i^m \chi_{a_i}$$

$$H_a \phi_a^m = \epsilon_a^m \phi_a^m$$

$$H_b \phi_b^m = \epsilon_b^m \phi_b^m$$

The overlap integral and other integrals between radicals are described by:

$$S_{mm} = \sum_i \sum_j C_i^m C_j^m \langle \chi_{a_i} | \chi_{b_j} \rangle$$

$$\langle \phi_a^m | 1/R_b | \phi_b^m \rangle = \sum_i \sum_j C_i^m C_j^m \langle \chi_{a_i} | \delta_j / R_{b_j} | \chi_{b_j} \rangle$$

$$\langle \phi_a^m \phi_a^m | \phi_b^m \phi_b^m \rangle = \sum_i \sum_j C_i^m C_j^m \langle \chi_{a_i}(1) \chi_{a_i}(1) | 1/r_{12} | \chi_{b_j}(2) \chi_{b_j}(2) \rangle$$

$$S_{mm} \langle \phi_a^m | 1/R_b | \phi_b^m \rangle = \sum_i \sum_j C_i^m C_j^m \langle \chi_{a_i} | \chi_{b_j} \rangle \langle \chi_{a_i} | \delta_j / R_{b_j} | \chi_{b_j} \rangle$$

By the use of these notations, the diagonal energy for the ground state may be given by:

$$\begin{aligned} E_{G,G} = & 2\epsilon_a^m - 2\langle \phi_a^m | 1/R_b | \phi_a^m \rangle + \langle \phi_a^m \phi_a^m | \phi_b^m \phi_b^m \rangle (1 - S_{mm}^2) + \sum_i \sum_j \frac{\delta_i \delta_j}{R_{a_i, b_j}} \\ & - 2S_{mm} \langle \phi_a^m | 1/R_b | \phi_b^m \rangle + 2S_{mm}^2 \langle \phi_a^m | 1/R_b | \phi_a^m \rangle + \langle \phi_a^m \phi_b^m | \phi_a^m \phi_b^m \rangle \end{aligned} \quad (4)$$

The diagonal energy for the molecular excited state relative to the ground state is calculated as:

$$\begin{aligned} E_{E,E} - E_{G,G} = & \epsilon_a^e - \epsilon_b^m - \langle \phi_a^e | 1/R_b | \phi_a^e \rangle + \langle \phi_a^m | 1/R_b | \phi_a^m \rangle + \langle \phi_a^e \phi_a^e | \phi_b^e \phi_b^e \rangle (1 - S_{ee}S_{mm}) \\ & - \langle \phi_a^m \phi_a^m | \phi_b^m \phi_b^m \rangle (1 - S_{mm}^2) - 2S_{me} \langle \phi_a^e | 1/R_b | \phi_b^m \rangle + 2S_{mm} \langle \phi_a^m | 1/R_b | \phi_b^m \rangle \\ & \pm \langle \phi_a^m \phi_a^e | \phi_b^m \phi_b^e \rangle (1 - S_{ee}S_{mm}) \pm \langle \phi_a^e \phi_b^m | \phi_a^e \phi_b^m \rangle \end{aligned} \quad (5)$$

If we use the following approximations, which are valid for a rough calculation:

$$C_i^{m^2} = C_i e^2, \quad S_{mm} \psi_a^m = S_{me} \psi_a^e \\ \langle \psi_a^e | 1/R_b | \psi_a^e \rangle = \langle \psi_a^m | 1/R_b | \psi_a^m \rangle \quad (6)$$

Equation (5) is reduced to:

$$E_{M,M\pm} - E_{G,G} = \epsilon_a^e - \epsilon_b^m \pm (\psi_a^m \psi_a^e | \psi_b^m \psi_b^e) (1 - S_{ee} S_{mm}) \pm (\psi_a^e \psi_b^m | \psi_a^e \psi_b^m) \\ \simeq \epsilon_a^e - \epsilon_b^m \pm (\psi_a^m \psi_a^e | \psi_b^m \psi_b^e) \quad (7)$$

The diagonal energy of the charge-transfer state relative to the ground state is evaluated as;

$$E_{CT,CT} - E_{G,G} = [(\psi_a^m \psi_a^m | \psi_a^m \psi_a^m) - (\psi_a^m \psi_a^m | \psi_b^m \psi_b^m)] (1 - S_{mm}^2) \quad (8)$$

The off-diagonal matrix element between the charge-transfer and molecular excited configurations and the ground configuration have been calculated. The results are:

$$E_{G,CT+} = \sqrt{2} [S_{mm} \epsilon_a - S_{mm} \langle \psi_a^m | 1/R_b | \psi_a^m \rangle - \langle \psi_a^m | 1/R_b | \psi_b^m \rangle \\ + (\psi_a^m \psi_a^m | \psi_a^m \psi_b^m) + S_{mm}/R_{a,b}] \quad (9) \\ E_{M\pm,CT\pm} = \sqrt{2} [\pm S_{me} \epsilon_a \mp S_{me} \langle \psi_a^m | 1/R_b | \psi_a^m \rangle \mp \langle \psi_a^m | 1/R_b | \psi_b^e \rangle \\ + (\psi_a^m \psi_a^e | \psi_a^m \psi_b^m) \pm (\psi_a^m \psi_a^m | \psi_a^m \psi_b^e) \pm S_{me}/R_{a,b}]$$

The off-diagonal element between the molecular excited and the ground state is set equal to zero since this term has already been diagonalized.

With a view to interpreting the spectra of the dimer and the crystal, we have performed semi-empirical calculations. Three configurations, the ground, the charge-transfer, and the molecular excited state, of the lowest energy of the  $y$  axis polarization have been taken into account, where the  $x$  and  $y$  axes have been chosen to be as shown in Fig. 1.

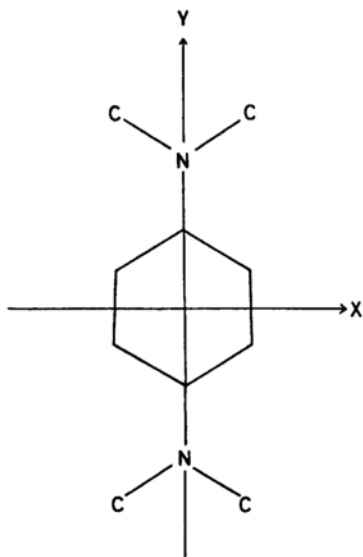


Fig. 1. The molecular axis of  $p$ -phenylenediamine.

The matrices for the symmetric ( $3 \times 3$ ) and the antisymmetric ( $2 \times 2$ ) states have been solved:

$$\begin{vmatrix} E_G & \beta & 0 \\ \beta & E_{CT+} & \beta' \\ 0 & \beta' & E_{M+} \end{vmatrix} = 0 \quad (10)$$

$$\begin{vmatrix} E_{CT-} & \beta'' \\ \beta'' & E_{M-} \end{vmatrix} = 0$$

Here the terms  $S_{G,CT}$ ,  $E$ ,  $S_{CT+,M+}$ ,  $E$ , and  $S_{CT-,M-}$ ,  $E$  are neglected in order to simplify the calculation. The actual calculation of the matrix elements is rather complicated; therefore, we have used semi-empirical values for the diagonal and off-diagonal elements. The diagonal element for the molecular excited state is taken from the peak of the absorption spectra in a solution. The energy of the charge-transfer state can be calculated by Eq. (8); however, the value is about 1 eV larger than the value envisaged from the dimer spectra in a solution. Therefore, we have used values which will fit the observed dimer spectra, 1.9 eV for the  $p$ -phenylenediamine cation dimer, 1.7 or 1.8 eV for Würster's red and 1.6 eV for Würster's blue dimers. The off-diagonal elements have been examined in detail; it is found that they are related to the overlap integrals between the relevant molecular orbitals. In order to make a spectral assignment and an interpretation, we have used several sets of tentative matrix elements,  $\beta$ ,  $\beta'$ , and  $\beta''$ ; the numerical values are tabulated in Table 1.

The results of the calculation are presented in

TABLE 1. MATRIX ELEMENTS FOR EQ (10)  
The units are in eV.

	$E_{CT}$	$E_M$	$\beta$	$\beta'$	$\beta''$
I	1.9	2.5	0.9	0.5	0.5
II	1.7	2.2	0.9	0.7	0.5
III	1.8	2.2	0.6	0.4	0.4
IV	1.6	2.1	0.25	0.1	0.05
V	1.6	2.1	0.23	0.1	0.1
VI	1.6	2.1	0.22	0.1	0.1
VII	1.6	2.1	0.11	0.05	0.05
VIII	1.6	2.1	0.10	0.05	0.04
IX	1.6	2.1	0.08	0.05	0.04

TABLE 2. ENERGY LEVELS AND WAVE FUNCTIONS

	Energy (eV)	G	CT <sub>+</sub>	M <sub>+</sub>	Energy (eV)	CT <sub>-</sub>	M <sub>-</sub>
I	-0.376	0.9225	-0.3802	0.0662			
	1.905	-0.3401	-0.7199	0.6050	1.617	0.8702	-0.4927
	2.866	0.1823	0.5806	0.7935	2.783	0.4927	0.8702
II	-0.419	0.9008	-0.4196	0.1121			
	1.517	-0.3829	-0.6452	0.6611	1.392	0.8520	-0.5241
	2.804	0.2050	0.6384	0.7419	2.508	0.5241	0.8520
III	-0.187	0.9533	-0.2978	0.0499			
	1.695	-0.2673	-0.7552	0.5985	1.553	0.8507	-0.5257
	2.492	0.1406	0.5839	0.7995	2.447	0.5257	0.8507
IV	-0.038	0.9885	-0.1513	0.0071	1.595	0.9951	-0.0985
	1.618	-0.1496	-0.9681	0.2008			
	2.120	0.0235	0.1996	0.9796	2.105	0.0985	0.9951
V	-0.0298	0.9909	-0.1342	0.0063			
	1.610	-0.1327	-0.9712	0.1981	1.595	0.9951	-0.0985
	2.120	0.0205	0.1971	0.9802	2.105	0.0985	0.9951
VI	-0.0247	0.9924	0.1225	0.0058	1.595	0.9951	-0.0985
	1.605	-0.1213	-0.9730	0.1965	2.105	0.0985	0.9951
	2.120	0.0185					
VII	-0.0075	0.9977	-0.0683	0.0016	1.597	0.9969	-0.0792
	1.6025	0.0681	0.9927	-0.0998	2.103	0.0792	0.9969
	2.1050	0.0052	0.0996	0.9950			
VIII	-0.006	0.9981	-0.0622	0.0148	1.597	0.9969	-0.0792
	1.601	0.0620	0.9931	0.0996	2.103	0.0792	0.9969
	2.105	0.0047	0.0994	0.9950			
IX	-0.0040	0.9988	-0.0498	0.0118	1.597	0.9969	-0.0792
	1.599	0.0497	0.9938	0.0992	2.103	0.0792	0.9969
	2.105	0.0038	0.0991	0.9951			

Tables 2 and 3. In Table 2 the wave functions are presented; by the use of these functions we can estimate the oscillator strength for each transition; their components are as shown in Table 3. Here the structure of the dimer is taken from the results of the crystal structure analysis.

The electronic absorption spectra of the Würster's dimer have been studied by several people; the results of Suzuki *et al.*<sup>2)</sup> are shown in Fig. 2. In this figure the spectra of *p*-phenylenediamine and Würster's blue cation are presented; the monomer band (curve 1) consists of R, X, and Y bands, while the dimer spectra (curve 2) show a new longer wavelength charge-transfer (CT) band and shifted R', X', and Y' bands. The splitting between the CT and R' bands and the intensities are greatly dependent on the magnitude of the intermolecular interaction. In Table 3 the calculated oscillator strengths are presented; it is there shown that the intensity ratio for the CT and R band is so sensitively dependent on the magnitudes of the matrix elements that we might be able to estimate the strength of the interaction accurately by comparing the observed and calculated values. In Fig. 3 the results of the calculation are illustrated; the appearance of

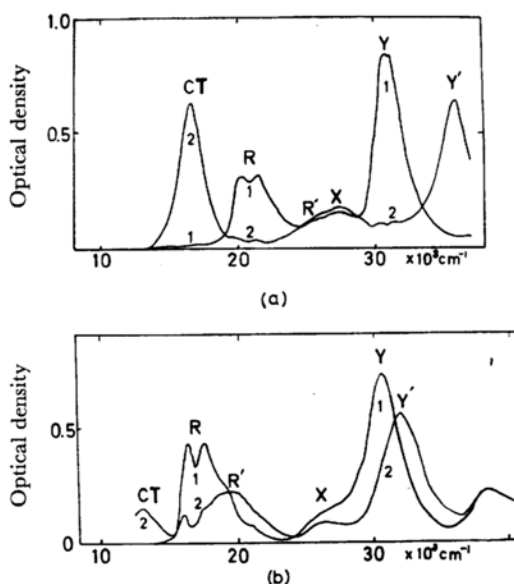


Fig. 2. Absorption spectra of (a) *p*-phenylenediamine cation and (b) Würster's blue perchlorate in solution. Curve 1 for the monomer and curve 2 for the dimer band. The data are taken from Uemura, Suzuki *et al.*<sup>2)</sup>

TABLE 3. TRANSITION ENERGIES AND ABSORPTION INTENSITIES

	Transition energies (eV)		Calculated intensities				The intensity ratio of the CT and the R' bands of the dimer	
	Calcd	Obsd	Transition moments (Å)			$f$ (oscillator-strength)	Calcd	Obsd
			$\mu$ (total)	$\mu$ ( $\perp$ )	$\mu$ ( $\parallel$ )			
I	1.99	2.04(a)	1.42	1.02	0.97	0.36	3.6 : 1	3.6 : 1 <sup>a)</sup>
	3.15	3.22	0.60	0.45	0.40	0.10		
II	1.81	1.85(b)	1.60	1.15	1.10	0.41	2.8 : 1	
	2.93	3.06	0.75	0.70	0.13	0.15		
III	1.74		1.18	0.78	0.88	0.22	2.4 : 1	1.6 : 1 <sup>b)</sup>
	2.63		0.58	0.50	0.31	9.09		
IV	1.63	1.61	0.62	0.53	0.40	0.055	0.5 : 1	0.59 : 1 <sup>c)</sup>
	2.14	2.36	0.73	0.05	0.73	0.11		
V	1.63		0.50	0.44	0.36	0.044	0.44 : 1	0.46 : 1 <sup>d)</sup>
	2.14		0.73	0.04	0.73	0.10		
VI	1.62		0.50	0.38	0.35	0.035	0.35 : 1	0.44 : 1 <sup>e)</sup>
	2.13		0.73	0.04	0.73	0.10		
VII	1.60		0.30	0.22	0.20	0.013	0.12 : 1	0.052 : 1 <sup>f)</sup>
	2.11		0.77	—	0.77	0.11		
VIII	1.60		0.27	0.20	0.19	0.01	0.09 : 1	
	2.11		0.77	—	0.77	0.11		
IX	1.60		0.23	0.16	0.17	0.007	0.06 : 1	0.063 : 1 <sup>g)</sup>
	2.11		0.77	—	0.77	0.11		

a) *p*-Phenylenediamine cation dimer in solution. Refs. 2 and 3.

b) Würster's red bromide in solution. Ref. 3.

c) Würster's blue bromide in crystal at room temperature. This work.

d) Würster's blue perchlorate in crystal at low temperature. Ref. 6.

e) Würster's blue perchlorate in solution. Refs. 2 and 6.

f) Würster's blue iodide in crystal at room temperature. This work.

g) Würster's blue perchlorate in crystal at room temperature. This work.

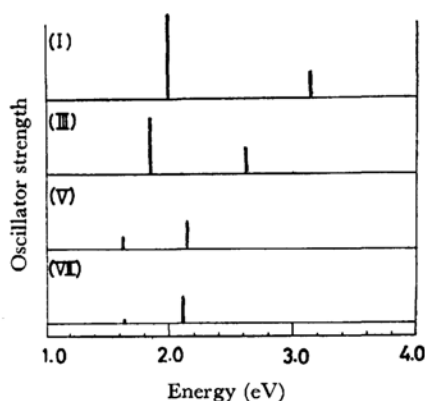


Fig. 3. The calculated energies and oscillator strength of the dimer spectra. The results shown in Tables 2 and 3 are presented; the numbers I, III, V and VII correspond to numbers in the tables.

the strong CT band and the large blue shift of the R band are intimately correlated with the intermolecular interaction. In Table 3 it may be seen that the case I corresponds to the *p*-phenylenediamine cation dimer in a solution, while the case II explains the Würster's red dimer and the case IV or V agrees well with Würster's blue dimer in a solution. The selected values of the off-diagonal matrix elements are quite reasonable from the point of view of steric repulsion, since the dimethyl group will hinder the stacking of the radicals.

In the next section several examples of crystal absorption will be presented, in which the change in the components of transition moments is exemplified by the intensity of the polarization spectra.

The ground-state stabilization energies, calculated as in Table 2, are intimately correlated with the singlet-triplet separation energies of the radical crystals. The experimental results on the magnetic susceptibilities of these crystals will be discussed in a separate paper.

### Crystalline Absorption Spectra

The crystals of Würster's blue perchlorate, blue iodide, blue bromide, and red bromide were synthesized by the method of Michaelis and Granick.<sup>9)</sup> Small crystals of microscopic size were selected under a polarization microscope for the spectral measurements, and the orientation of the crystalline axis was determined by taking X-ray photographs. The spectra were measured using a microspectrophotometer consisting of a Carl Zeiss monochromator and an Olympus microscope. Some of these crystals are unstable at room temperature; therefore, the measurements were carried out as soon as possible after preparation.

i) **Würster's Blue Perchlorate.** The crystals of Würster's blue perchlorate show a brownish metallic reflection, hexagonal or square in rhomb shape. The crystalline structure has been analysed by Turner and Albrecht;<sup>10)</sup> their results, as yet unpublished, have been confirmed in this laboratory. The crystal belongs to the orthorhombic system of the  $P_n2_n$  space group with lattice constants of  $a=5.98$ ,  $b=10.21$ , and  $c=10.23$  Å. It includes two molecules in a unit cell; the projection of molecules onto the  $ac$  plane is depicted in Fig. 4. There were two crystalline types, the developing  $ac$  plane and the developing  $ab$  plane. The crystalline absorption measured on the  $ac$  plane is shown in Fig. 5; it is remarkable that the charge-transfer band is very weak in crystals. It appears at  $11500\text{ cm}^{-1}$  with its polarization along the  $a$  axis. In Fig. 6 another spectra with an  $ab$  plane develop-

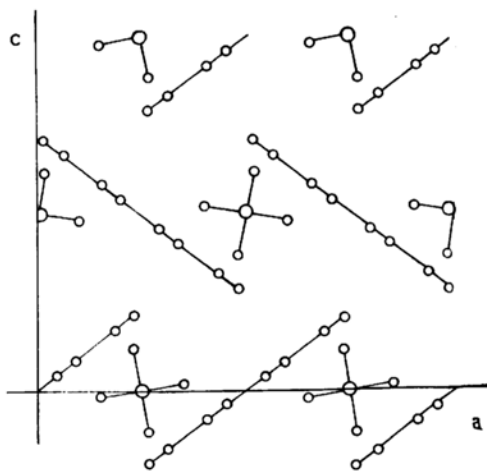


Fig. 4. Projection of Würster's blue perchlorate crystal onto the  $ac$  plane.

9) L. Michaelis and S. Granick, *J. Am. Chem. Soc.*, **65**, 1747 (1943).

10) J. D. Turner and A. C. Albrecht, unpublished results (1955); see *J. Chem. Phys.*, **39**, 2321 (1963). We are grateful to Professor Albrecht for his communication on his unpublished result.

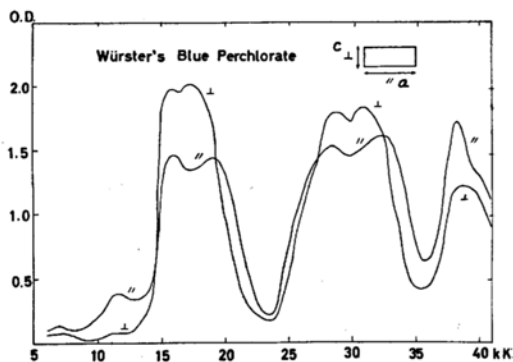


Fig. 5. The crystalline absorption spectra of Würster's blue perchlorate on the  $ac$  plane.

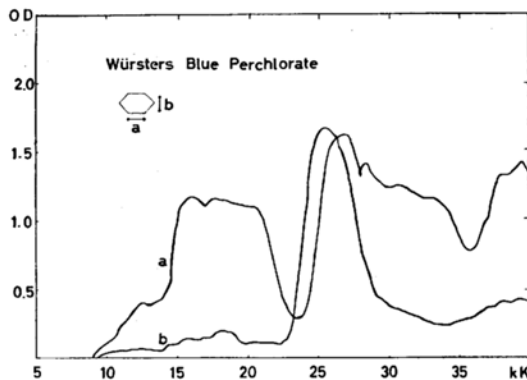


Fig. 6. The crystalline absorption spectra of Würster's blue perchlorate on the  $ab$  plane.

ing is presented; the band has no component along the  $b$  axis. These two results have shown that the charge transfer band is polarized along the direction of the  $a$  axis; in this direction the lines connecting the centers of the stacked radicals are parallel. In view of the theoretical results, the charge-transfer transition should have a polarization parallel to the line connecting the center of the donor and the acceptor molecules. In the present system the Würster's ion acts as both the electron donor and the acceptor by itself; therefore, the polarization of the charge transfer band may be expected to be found only along the  $a$  axis. Therefore the weak  $11500\text{ cm}^{-1}$  band is confirmed to be predominantly charge-transfer in character. It is very interesting that, in a solution at a lower temperature, the intensity of the charge-transfer band of the dimer was larger than in a crystal. The fact that the intensity of the charge-transfer band is greatly dependent on the overlapping of pi-electrons suggests that the stacking of radicals might be more effective for the dimer in a solution than in a crystal. Recent experiments by Anderson<sup>11)</sup> and Sakata and Nagakura<sup>6)</sup> have shown that the intensity of the charge transfer band increases

11) G. R. Anderson, *J. Chem. Phys.*, **47**, 3853 (1967).

markedly below the transition point of the crystal. However, at room temperature, the crystalline spectrum is much like the spectrum of the radical monomer in a solution; therefore, the succeeding band may be regarded as representing the polarization characteristics of the radical excited states. In the 15000–20000  $\text{cm}^{-1}$  region, the R-band is not observed along the  $b$  axis on the  $ab$  plane. If the polarization of this band is the short axis of the radical (the  $x$  axis in Fig. 1), it should be very strong along the  $b$  axis. The observed result is contrary to this prediction; therefore, the transition moment must be on the long axis ( $y$  axis). This is in harmony with our theoretical results presented in a separated paper.<sup>8)</sup> The observed dichroic ratio,  $I_a : I_c$  was 0.7 : 1.0, while the calculated value, assuming the long-axis polarization, is 1.3 : 1.0. The agreement is not perfect; however, the last choice of a polarization vertical to the benzene ring is not acceptable since the R-band is undoubtedly a pi-pi transition and so its transition moment must be on the plane of the benzene ring. The deviation of the dichroic ratio might result from a mixing with other excited states. In the calculation presented in Table 3, the intensity ratio for the CT and R band is evaluated. The observed value is 0.063 : 1, while the value calculated by means of the parameter (IX) is 0.06 : 1. This agreement suggests that interaction parameters as small as  $\beta = 0.08$  eV are valid for this crystal.

In the  $b$  axis spectrum a peak is observed at 25500  $\text{cm}^{-1}$ , it corresponds to the X-band in the monomer spectrum. This band is not observed along either the  $a$  axis or the  $c$  axis; therefore, its polarization is confirmed to be the short axis of the radical. This result is also consistent with our prediction of the sequence of the excited state energy levels. In the range of 26000–34000  $\text{cm}^{-1}$  a very broad band is observed along the spectra of both the  $a$  and  $c$  axes. This is correlated to the Y-band in a solution, and the polarization may safely be regarded as being to the long axis of the radical. In a higher energy region at about 38000  $\text{cm}^{-1}$  another peak is observed; it is the W-band, and its polarization is also the long axis of the radical. Summarizing these results, it may be concluded that the polarizations of the radical excited states for R, Y, and W bands are  $y$  axis, while that for the X-band is  $x$  axis. Although the longest wavelength charge-transfer band is not as prominent in crystals, its polarization is perfectly on the line connecting the radicals, consistent with the theoretical results, shown in Table 3.

**ii) Würster's Blue Iodide.** The crystal structure of Würster's blue iodide is very much like that of blue perchlorate; the structure has recently been determined by De Boer, Vos, and Huml.<sup>12)</sup> The

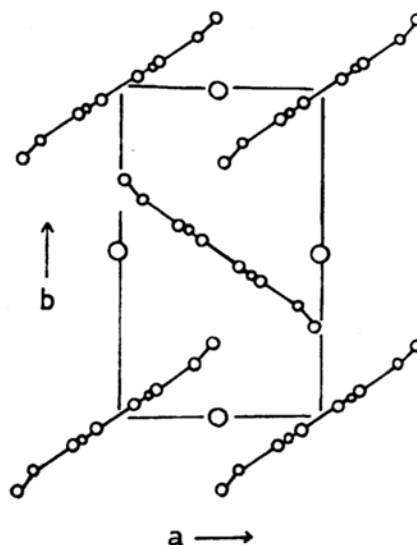


Fig. 7. Projection of Würster's blue iodide crystal onto the  $ab$  plane.

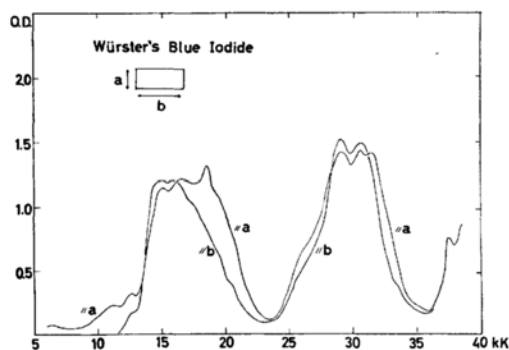


Fig. 8. The crystalline absorption spectra of Würster's blue iodide on the  $ab$  plane.

crystal belongs to the orthorhombic system; the space group is  $Pnmm$  with  $Z=2$ . The unit cell dimensions are  $a=5.919$ ,  $b=9.855$ , and  $c=9.901$  Å. The projection of molecules onto the  $ab$  plane is shown in Fig. 7.

The crystalline absorption spectrum has been measured on the  $ab$  plane (Fig. 8). Although the inclination of the long axis to the  $a$  axis is decreased by  $2.5^\circ$  as compared to Würster's blue perchlorate, the spectrum is very close to the  $ac$  plane spectrum of perchlorate. The charge-transfer band is found at 11200 and 12500  $\text{cm}^{-1}$ . The theoretical analysis presented above showed that the transition moment for this band is on the  $a$  axis of the crystal. The broad R-band is observed around the 14000–21000  $\text{cm}^{-1}$  region and it showed several peaks which may be supposed to be due to the vibrational progressions. The X band is not obvious on this plane, but a little shoulder was found at 26000  $\text{cm}^{-1}$ . The Y band is observed in the 28000–33000  $\text{cm}^{-1}$

12) J. L. De Boer, A. Vos and K. Huml, *Acta Cryst.*, **B24**, 542 (1968).

range; the polarization results are consistent with the previous conclusions drawn from the perchlorate crystalline spectrum.

In the iodide crystal the intensity ratio for the CT and R bands is found to be 0.052 : 1. This result suggests that the weakest interaction parameters will be valid for this crystal; however, the magnetic results show that the interaction might be slightly larger than in the perchlorate crystal. The overlap integral between the highest occupied orbitals will be discussed in the last section; it supports the idea of rather bigger parameters for this crystal.

Different crystalline modifications of Würster's blue iodide have been reported by Hughes and Hush.<sup>13)</sup> In this experiment it has also been found that the other crystalline form is sometimes found in crystals obtained from a methanol solution. However, these crystals are rather unstable and rare; therefore, this form is not reported on in this paper.

**iii) Würster's Blue Bromide.** The crystal of Würster's blue bromide was obtained as brown-black needles, and a small, thin crystal was dark blue in light polarized parallel to the elongation axis and pale reddish in light polarized in the perpendicular direction. The crystal structure is now under investigation in this laboratory, while the space group and the cell constants have been determined to be as follows:

Crystal Data: Orthorhombic,  $Cmcm$ ,  $a=9.54$ ,  $b=19.27$ ,  $c=7.03$  Å,  $z=4$ .

The preliminary crystal structure results show that the elongation axis is the  $c$  axis, the benzene ring is perpendicular to the  $c$  axis, and the  $y$ -axis of the radical is parallel to the  $b$  axis. The projection of molecules onto the  $ab$  plane is shown in Fig. 9, and the projection onto the  $bc$  plane, in Fig. 10. The crystalline absorption spectra have been measured on the  $ac$  and  $bc$  planes by a polarized light; the results are shown in Figs. 11 and 12. In the range of 8000–15000  $\text{cm}^{-1}$ , where a charge-

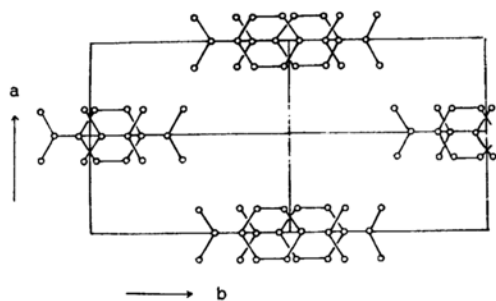


Fig. 9. Projection of Würster's blue bromide crystal onto the  $ab$  plane by the preliminary X-ray results.

13) G. K. Hughes and N. S. Hush, *J. Proc. Roy. Soc. N.S.W.*, **81**, 48 (1947).

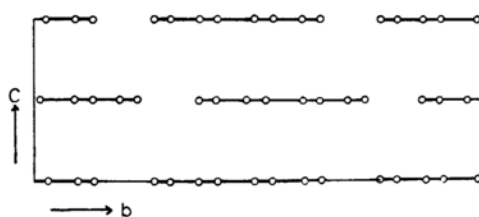


Fig. 10. Projection of Würster's blue bromide crystal onto the  $bc$  plane by the preliminary X-ray results.

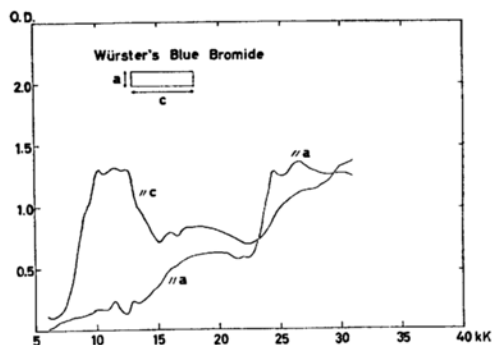


Fig. 11. The crystalline absorption spectra of Würster's blue bromide on the  $ac$  plane.

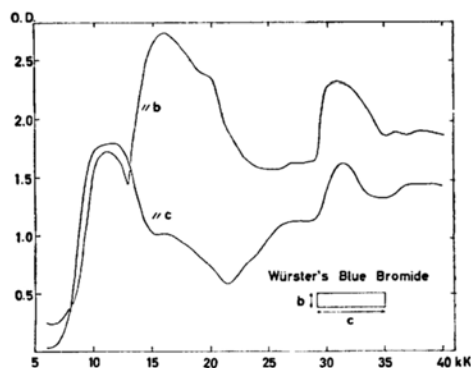


Fig. 12. The crystalline absorption spectra of Würster's blue bromide on the  $bc$  plane.

transfer transition is expected, a broad peak is observed along both the  $b$  and  $c$  axes, but not along the  $a$  axis, where a weak absorption tail is observed. The transition moment of the charge-transfer transition is on the line connecting the stacked radicals; therefore, it has components along the  $c$  and  $b$  axes, but not along the  $a$  axis. The observed intensity ratio for the CT and R bands is about 0.55 : 1, while the calculated values are 0.35 : 1–0.5 : 1. The values of the intensity ratio for the perpendicular ( $c$  axis) and parallel ( $b$  axis) directions are 1.35 : 1 for the CT band and the calculated values are 1.2 : 1–1.7 : 1, in fairly good agreement with the observed values.

The next strong band is observed particularly along the  $b$  axis in the 15000–23000  $\text{cm}^{-1}$  region;



it may be regarded as an R-band mixed to some extent with the CT band. The R-band originally has its own polarization parallel to the long axis of the radical; however, the mixing with the charge-transfer configuration will result in some component along the out-of-plane of the benzene ring. The observed weak peak at  $18000\text{ cm}^{-1}$  in the  $c$  axis direction may be explained on this basis. The intensity ratio observed is  $0.02 : 1$  for the  $c$  axis-to- $b$  axis polarization, while the value calculated by the model IV is  $0.005$ .

In the  $26000\text{ cm}^{-1}$  region the next peak is found for the  $a$  axis spectrum; it may safely be assigned to the short-axis polarized X band.

As has been discussed above, if we increase the intermolecular interaction, the intensity of the charge-transfer band will be increased and the splitting between the CT and R bands will be enlarged. Judging by this criterion, the strength of the interaction in the Würster's blue bromide crystal is an intermediate case compared to the blue perchlorate and red bromide.

Another crystalline form of Würster's blue bromide has been obtained by rare chance. It was transparent when observed along the elongation axis and dark black in the perpendicular direction. The spectra have been recorded, but the crystalline data have not yet been obtained; therefore, we will not here discuss the spectral results in detail.

**iv) Würster's Red Bromide.** The crystals of Würster's red bromide (*N,N*-dimethyl-*p*-phenylenediamine bromide) have been prepared as dark green needles. The thin crystals are dark green in light polarized parallel to the elongation axis, and pale green in light polarized in the perpendicular direction. The crystalline structure has been analyzed in this laboratory<sup>7)</sup>; it has been found that the radicals are stacked at equal distances from each other, with unusually short interplanar spacing in the one-dimensional column. The intermolecular interaction is extraordinary large in this crystal, and the spectra are quite different from that of other types of Würster's salt.

The thin crystal develops the  $ac$  plane; its absorption spectra have been measured by a polarized light. The spectra are presented in Fig. 13, while the projection of radicals on the  $ac$  plane is shown in Fig. 14. The projection on the  $ab$  plane is also

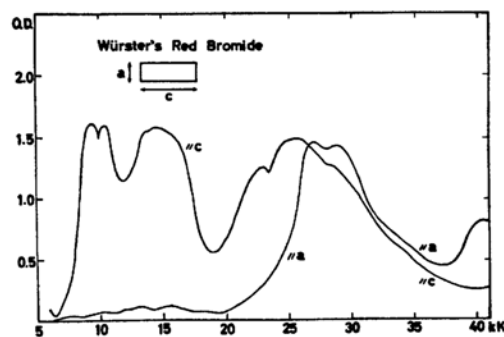


Fig. 13. The crystalline absorption spectra of Würster's red bromide on the  $ac$  plane.

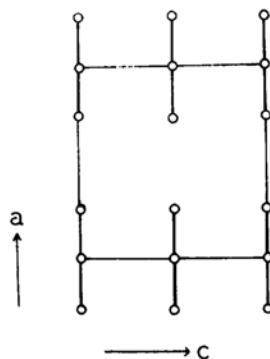


Fig. 14. Projection of Würster's red bromide crystal onto the  $ac$  plane.

depicted in Fig. 15. The broad strong bands are observed along the  $c$  axis in the  $7000\text{--}18000\text{ cm}^{-1}$  region, which consists of two prominent peaks. The polarization of this band is definitely in the direction of the out-of-plane of the benzene ring; therefore, this band must be charge-transfer in origin. The next broad band observed along the  $c$  axis starts at  $18000\text{ cm}^{-1}$  and extends to the  $40000\text{ cm}^{-1}$  region. The polarization characteristic of this band may be understood if we assume that extensive mixing occurs between the charge transfer and the R-excited configurations. Since the long axis of the radical is parallel to the crystalline  $b$  axis, the  $R'$  band can not be observed along the  $c$  axis unless the configurational interaction with the charge transfer state takes place. The calcula-

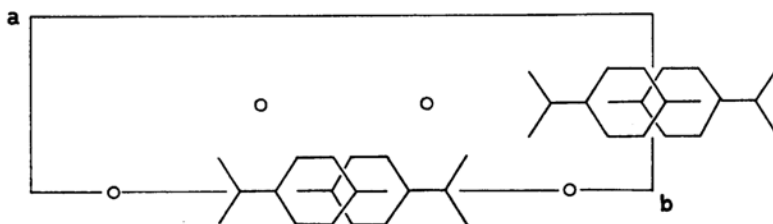


Fig. 15. Projection of Würster's red bromide crystal onto the  $ab$  plane.

tions of the previous section showed that the R' band has a fairly strong component in out-of-plane direction as a result of the large mixing of the CT and R states. The intensity ratio for the out-of-plane direction of the CT and R' bands is calculated to be 1.5 : 1, while the observed value is 0.9 : 1.

Although the first charge-transfer band might be accompanied by several vibrational progressions, it is quite noteworthy that it shows two peaks, one in the 9500  $\text{cm}^{-1}$  region and another in the 13500  $\text{cm}^{-1}$  region. The splitting of this band is an indication of the strong radical-radical interaction in the one-dimensional column in the crystal. A possible explanation of this band splitting will be given in the last section.

The short-axis polarized band is observed along the *a* axis, and it appears in the 25000—33000  $\text{cm}^{-1}$  region. It is assigned to the X band; this is in conformity with the previous findings on other Würster's salts.

**v) *p*-Phenylenediamine Bromide.** The crystals of *p*-phenylenediamine bromide have been obtained as dark brown microcrystals. The crystalline data could not be obtained with this crystal, however, since it is not large enough for X-ray examination. The crystalline absorption spectra have been measured by a polarized light for the elongation axis and in the perpendicular direction (Fig. 16).

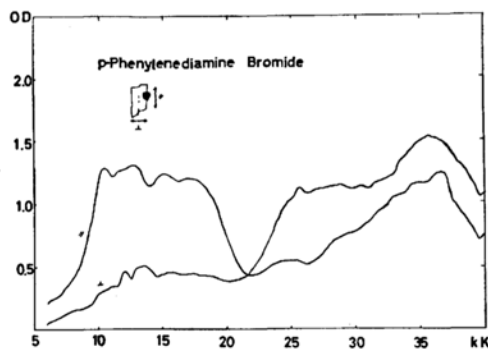


Fig. 16. The crystalline absorption spectra of *p*-phenylenediamine bromide.

The crystalline absorption bands are similar to that of Würster's red bromide, but it is remarkable that the absorption bands are broader than those of any other Würster's crystals. This means that the intermolecular interaction is the largest in this series of radical salts. This finding is supported by the experimental results<sup>2,3</sup>) on the solution and by the calculation, and it is consistent with the steric considerations. The crystal structure is not yet known; therefore, our results will not be discussed further.

**Interaction between Radicals and Crystalline Spectra.** The effects of the intermolecular interaction are most significant in radical salt crystals than in any other type of molecular crystals

since the unpaired electron on each radical will make a bonding between the radicals. The covalent force bind the radicals close to each other, while the exchange repulsion of the closed-shell electrons, including the so-called steric repulsions, increase the radical-radical distances. The positive charge carried on each ion is also repulsive in the present system. The analysis of these intermolecular forces might be difficult, however, the actual crystal structure represents a counterbalance of these several composite forces.

However, the tendency toward binding is shown by the formation of the radical dimer in a solution. It has been observed in Würster's radical, the ethylphenazyl radical,<sup>1-3</sup>) the tetracyanoquinodimethane anion,<sup>14</sup>) and pyridinium radicals<sup>15</sup>) to form dimers in solutions, particularly at low temperatures. Characteristic of the aromatic radical dimer system is the appearance of a new absorption band in the longer-wavelength region. This band appears regardless of the charges on the radical; therefore, interaction between the unpaired electrons must be essential for the appearance of the new band. The interaction with the singly-occupied orbital is greatly dependent on the relative interatomic distances and orientations. Therefore, the present system of Würster's radicals will provide typical cases to be investigated, cases where the interplanar spacings are somewhat different from crystal to crystal: spectral and crystallographic data have accordingly been assembled.

The origin of the new band has been explained above in terms of the charge-transfer mechanism. Although we believe that the Heitler-London approach is most valid for discussions of the inter-radical electronic interactions, for the stronger dimers at shorter intermolecular distances the molecular orbital method is also illuminating. The appearance of the longer-wavelength absorption band can be explained simply in terms of a transition from the bonding to the antibonding orbital (*cf.* Fig. 17).<sup>3</sup>) The inclusion of the ionic structures and

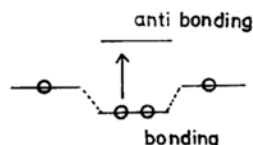


Fig. 17. Molecular orbital description of the radical-radical interaction.

the appearance of the new band which is polarized in the out-of-plane direction are naturally predicted by this method. However, the defect of this

14) R. H. Boyd and W. D. Phillips, *J. Chem. Phys.*, **43**, 2927 (1965).

15) M. Itoh and S. Nagakura, *J. Am. Chem. Soc.*, **89**, 3959 (1967).

TABLE 4. OVERLAP INTEGRALS BETWEEN RADICALS

	Würster's red bromide	Würster's blue bromide	Würster's blue perchlorate	Würster's blue iodide
$S_{mm}$	$0.205 \times 10^{-1}$	$0.344 \times 10^{-2}$	$0.121 \times 10^{-2}$	$0.247 \times 10^{-2}$
$S_{ee}$	$-0.166 \times 10^{-2}$	$-0.69 \times 10^{-4}$	$0.297 \times 10^{-2}$	$-0.266 \times 10^{-2}$
$S_{me}$	$0.404 \times 10^{-2}$	$-0.325 \times 10^{-2}$	$0.195 \times 10^{-2}$	$0.268 \times 10^{-2}$
Positions of radicals	(0, 0, 0) and (0, 0, $\frac{1}{2}$ )	(0, 0, 0) and (0, 0, $\frac{1}{2}$ )	(0, 0, 0) and (1, 0, 0)	(0, 0, 0) and (1, 0, 0)

TABLE 5. THE INTERACTION MATRIX ELEMENTS AND THE OVERLAP INTEGRALS

	Würster's blue perchlorate	Blue iodide	Blue bromide	Red bromide
$\beta$ (eV)	0.08 (IX)	0.11 (VII)	0.22 (IV)	0.9 (II), 0.6 (III)
$S_{mm}$	0.0012	0.0025	0.0034	0.021

approach is its incapability of explaining the appearance of a weak charge-transfer band in nearly the same energy region. Therefore, the molecular orbital method is limited only for cases of the stronger interaction.

According to both theories the strength of the electronic interaction can be roughly estimated by means of the magnitude of the overlap integrals. The overlap integrals of the radical pair evaluated for several crystals are shown in Table 4. The atomic orbitals used are those of the Hartree-Fock AO of Clementi<sup>16)</sup> and the calculations were carried out at the Computation Center of the University of Tokyo. The results of the calculation have also been compared with the parameters of the interaction estimated in the previous sections. They are listed in Table 5 where it is found that a rough correlation exists between these values.

The intensities of the CT band and the R band are mostly determined by the extent of the mixing of the CT configuration with other configurations. Each state can be described as a mixture of three configurations,  $\Psi_G$ ,  $\Psi_{CT}$ , and  $\Psi_M$ , as Table 2 shows. The transition moments consist of terms proportional to  $\langle \Psi_{CT} | \mathbf{r} | \Psi_{CT} \rangle$  and  $\langle \Psi_G | \mathbf{r} | \Psi_M \rangle$ ; therefore, the directions of the transition moments are determined by the extent of the mixing of these configurations. In Würster's blue perchlorate, where the overlap integral is the smallest, the intensity of the charge-transfer band is the weakest. Würster's blue bromide shows an intermediate case in both absorption intensity and calculated overlap integral. In Würster's red bromide the charge-transfer band is extraordinarily large and the overlap integral is the largest.

The appearance of the broad and doublet structure of the CT band of the red bromide and *p*-phenylenediamine bromide crystals is puzzling; it must be intimately connected with the large electron overlap between the radicals. These absorp-

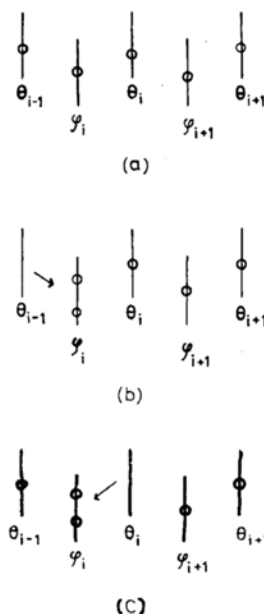


Fig. 18. Unpaired electrons on radicals in the one-dimensional crystal.

(a) ground configuration (b) left to right charge transfer state (c) right to left charge transfer state.

tion band are, of course, associated with the vibrational structures; however, we believe that the large breadth might be due to an electronic effect. Now let us discuss this effect by considering only the unpaired electrons on each radical, as is shown in Fig. 18. There are two sites in the one-dimensional radical column in a unit cell; we will denote the unpaired orbitals in the  $i$ th cell by  $\varphi_i$  and  $\theta_i$ . The wave function for the ground configuration (no charge-transfer structure) is:

$$\Phi_0 = \frac{1}{\sqrt{2N!}} \prod_{i=0}^N \varphi_i(i) \theta_i(2i)$$

16) E. Clementi, *IBM Journal*, **9**, 2 (1965).

where  $N$  is the number of unit cells considered and where  $\alpha$  is the antisymmetrizer. There are two kinds of charge-transfer states; one is from the left site to the right site, and the other is from right to left. The crystalline charge-transfer states which satisfy the requirements of translational symmetry are given by:

$$\Psi_{CT}(\rightarrow, \pm) = \frac{1}{\sqrt{2}} \sum_i \left( \frac{\Phi_0}{\theta_{i-1}} \varphi_i \pm \frac{\Phi_0}{\varphi_i} \theta_i \right)$$

$$\Psi_{CT}(\leftarrow, \pm) = \frac{1}{\sqrt{2}} \sum_i \left( \frac{\Phi_0}{\theta_i} \varphi_i \pm \frac{\Phi_0}{\varphi_i} \theta_{i-1} \right)$$

There are also symmetric and antisymmetric combinations; therefore, four different kinds of excited states altogether must be considered. The plus combinations are optically active along the  $c$  axis in Fig. 18, while minus combinations are active along the  $b$  axis. The right- and left-directed charge-transfer states which have degeneracy will combine again; only the two states shown below are optically active, being active along the  $b$  and  $c$  axes respectively.

$$\Phi_{CT}(a, \perp) = \frac{1}{\sqrt{2}} [\Psi_{CT}(\rightarrow, -) + \Psi_{CT}(\leftarrow, -)]$$

$$\Phi_{CT}(a, //) = \frac{1}{\sqrt{2}} [\Psi_{CT}(\rightarrow, +) - \Psi_{CT}(\leftarrow, +)]$$

The inactive excited states are obtained by the following combinations;

$$\Phi_{CT}(i, \perp) = \frac{1}{\sqrt{2}} [\Psi_{CT}(\rightarrow, -) - \Psi_{CT}(\leftarrow, -)]$$

$$\Phi_{CT}(i, //) = \frac{1}{\sqrt{2}} [\Psi_{CT}(\rightarrow, +) + \Psi_{CT}(\leftarrow, +)]$$

Now let us concern ourselves with the  $c$  axis polarized spectrum. Here, there are two relevant states,  $\Phi_{CT}(a, //)$  and  $\Phi_{CT}(i, //)$ . The splitting of these two states is given by the off-diagonal element,  $\langle \Psi_{CT}(\rightarrow, +) | H | \Psi_{CT}(\leftarrow, +) \rangle$ . This element has not terms proportional to the first order in the nearest neighbor electron overlap. However, the electron-electron interaction of a dipolar type appears and the splitting is given by:

$$\langle \varphi_i(1) \theta_{i-1}(1) | 1/r_{12} | \varphi_i(2) \theta_i(2) \rangle.$$

The numerical estimation of this value gives a stabilization of the active state amounting to 0.75 eV ( $6000 \text{ cm}^{-1}$ ) relative to the inactive state. The splitting of the band observed in the crystalline spectra is of just the same order of magnitude; therefore, it is conceivable that the inactive state appears by means of the intensity borrowing through the vibrational or other kinds of perturbations.

The alternative approach to the understanding of the spectral characteristics is by the band theory, which is an extension of the molecular orbital method. We believe, however, that it will be inadequate for the present system of crystals, and so it will not be discussed further.

The authors acknowledge to the Ministry of Education for the research grant.